Propagation in photonic crystal coupled-cavity waveguides with discontinuities in their optical properties

Ben Z. Steinberg and Amir Boag

School of Electrical Engineering, Faculty of Engineering, Tel-Aviv University, Tel-Aviv 69978, Israel

Received September 20, 2005; revised December 6, 2005; accepted January 12, 2006; posted March 8, 2006 (Doc. ID 64847)

An analytical model for propagation through and reflection from a discontinuity in coupled-cavity waveguides (CCWs) (also known as coupled-resonator optical waveguides—CROW) is developed. The theory is based on a modification of the tight-binding theory for propagation in nonuniform structures. Explicit analytic expressions for the reflection and transmission coefficients are obtained. These expressions resemble in form and structure the well-known Fresnel coefficients, with the traditional wave impedance parameter replaced by the device bandwidth. Matching of two uniform CCWs with the use of an intermediate serial section is also discussed, and an analogy to the well-known quarter-wavelength plate is pointed out. © 2006 Optical Society of America

OCIS codes: 130.2790, 230.5750.

1. INTRODUCTION

Much attention has been devoted recently to the theory and applications of the coupled-cavity waveguide (CCW), also known as the coupled-resonator optical waveguide, or CROW. This device consists essentially of an array of weakly coupled high-Q optical resonators, along which a light signal can propagate.[1–3] Schematic examples of this device are shown in Fig. 1.

In one realization, the CCW is a linear array of equally spaced local defects, situated within an otherwise perfect photonic crystal (PhC). Each local defect serves as a microcavity possessing a local resonant mode (trapped mode) with a resonant frequency within the bandgap of the background PhC. Propagation along the CCW is based on tunneling of radiation from one microcavity to the next. When the microcavities are all identical, possessing the same resonant frequency ω_0, the resulting CCW constitutes a narrowband low-group-velocity optical transmission device, with central frequency ω_0. The transmission bandwidth and group velocity decrease very fast as the intercavities' distance increases. These properties have been derived using tight-binding perturbation theory[1,3] and verified both experimentally[2] and against numerical simulations.[3] The case of a CCW possessing nonidentical microcavities and structural disorder has been studied[4] using cavity perturbation theory in conjunction with the tight-binding theory. Another realization of the CCW that does not require the presence of a PhC background environment has also been suggested.[5] Here, an array of weakly coupled microring optical resonators is used. Although at first glance this structure looks quite different from that realized in a PhC, and the analysis is also based on the transfer-matrix approach, the propagation physics is essentially the same as well as the resulting dispersion relations.

Because of the appealing properties of the CCW (e.g., the ability to design *a priori* the transmission frequency, bandwidth, and group velocity), it has been proposed as a potential candidate for various applications in optical communication systems. This includes, for example, filtering and routing and add–drop devices.[1,3–5] As it consists of a series of high-Q resonators it can be used in applications where a high field intensity is required such as soliton optics[6] and higher harmonic generation.[7] Because of the low group velocity, it has also been suggested as a potential candidate for optical storage and optical delay lines.[8–10] On a different track of applications, the CCW has been suggested also as a candidate for the design of ultracompact optical gyroscopes.[11]

In view of this potential wealth of applications, it is anticipated that assemblies of mutually connected CCWs can become inherent in many optical systems. Then the propagation through a variety of CCWs and the associated back reflection and multiple reflections may lead to mismatch and insertion loss that obviously affects the overall system performance. Thus, the purpose of the present work is to study the propagation in a CCW that consists of two semi-infinite, different uniform CCWs, situated in series as shown schematically in Fig. 1. The combined CCW can be viewed as a single CCW with property discontinuity occurring at the passage from the microcavity numbered by $k=0$ to that numbered by $k=1$. It is shown that relatively simple analytic expressions for the reflected and transmitted optical signals can be derived, and their structure resembles that of the well-known Fresnel reflection and transmission coefficients. Furthermore, our new results indicate an intimate relation between the conventional notion of wave impedance and the bandwidth of a CCW. Hence, this structure serves as a paradigm case—a basic building block from which the behavior of more complicated networks can be inferred. For example, we show that the theory developed here can be used to match two serially connected CCWs by inserting a finite-length intermediate section. In some

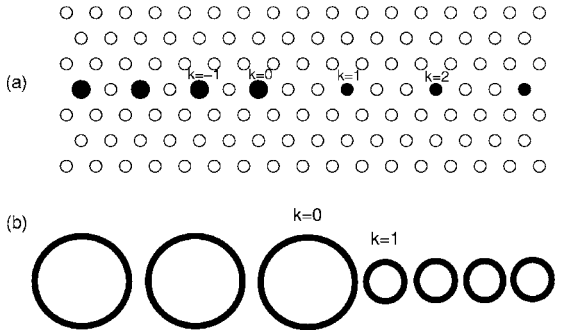

Fig. 1. Two examples for a system of two different CCWs connected in series. (a) Realization in photonic crystal. Local defects are shown by solid circles. The CCWs may differ in the local defect form and intercavity spacing, thus differing in both central frequency and bandwidth. (b) Realization using an array of microring resonators.

simplified cases (when the two CCWs have the same central frequency) perfect matching can be achieved using a single-cavity intermediate section, and the corresponding parameters resemble the well-known quarter-wavelength plate condition.

To study the combined structure, we start with the nonuniform CCW model developed previously.[4] The original motivation of this work has been to study the effect of structural disorder, which is essentially random. However, the general framework developed there holds also for structures possessing variations that are deterministic and limited to local regions. We emphasize that although most of the specific figures and examples are inclined toward the PhC-based CCW, the mathematical expressions for transmission and reflection coefficients, as well as the general resemblance to well-known propagation phenomenology articulated above, are general and hold for other CCW configurations such as the microring system—see Fig. 1(b). The theory developed here applies to CCWs in two-dimensional (2D) (e.g., a structure in the x,y plane that is invariant in z, or alternatively the microring system) and three-dimensional (3D) configurations. It should also be noted that the 2D realizations of PhC structures and high-Q microcavities in dielectric slabs, studied by several research groups,[12–15] offer another practical realization of CCWs. Here, the microcavity transverse confinement is provided by the periodic structure in the plane, while the vertical confinement is provided by the slab guiding (total internal reflection). It has been shown that for the frequency range that corresponds to the lowest guided mode in the slab, the properties of such structures can be approximated by an ideal 2D structure using the effective index approach.[12] Since the basic physical mechanism as well as the dispersion equation of a CCW in these structures are essentially the same as those of the perfect 2D and 3D cases, the theory developed here applies to these cases as well.

The structure of the paper is as follows. In Section 2 we present the basic formulation that applies to a nonuniform CCW and discuss some of its properties needed for subsequent derivations. In Section 3 we develop the reflection and transmission coefficients due to the properties' discontinuity occurring at a single location along the CCW. In Section 4 we use these results to demonstrate matching between two CCWs using an intermediate CCW section. The theory is checked against numerical examples in Section 5, and concluding comments are given in Section 6.

2. FORMULATION

Let $\epsilon_b(\mathbf{r})$ be the relative permittivity of the PhC, including possible random inaccuracies, but excluding the defect sites. Thus, $\epsilon_b(\mathbf{r})$ describes a perfectly periodic PhC superimposed on which is some noisy structure that represents the random inaccuracy. Let $\epsilon_{d_n}(\mathbf{r})$ and $\mathbf{H}_n(\mathbf{r})$ represent the aforementioned inaccurate crystal including the nth microcavity only and the associated mode magnetic field, respectively. Its resonant frequency is ω_n. For a perfectly uniform CCW we have $\epsilon_{d_n}(\mathbf{r})=\epsilon_{d_0}(\mathbf{r}-n\mathbf{b})$, where $\mathbf{b}$ is the intercavity spacing vector.[3] We define

$$d_n(\mathbf{r}) = \frac{1}{\epsilon_{d_n}(\mathbf{r})} - \frac{1}{\epsilon_b}(\mathbf{r}), \tag{2.1}$$

which represents the single defect corresponding to the nth microcavity in its true position. Note that due to random structure inaccuracies and/or structure variation, the shift-invariance property $d_n(\mathbf{r})=d(\mathbf{r}-n\mathbf{b})$ does not hold. Let $\epsilon_r(\mathbf{r})$ be the relative permittivity of the entire PhC structure, including the random inaccuracies and the linear array of defects that forms our two CCWs. We have

$$\frac{1}{\epsilon_r(\mathbf{r})} = \frac{1}{\epsilon_b(\mathbf{r})} + \sum_n d_n(\mathbf{r}). \tag{2.2}$$

In accordance with the traditional notations,[16] we define the operators

$$\boldsymbol{\Theta} \equiv \boldsymbol{\nabla} \times \frac{1}{\epsilon_r(\mathbf{r})} \boldsymbol{\nabla} \times, \quad \boldsymbol{\Theta}^b \equiv \boldsymbol{\nabla} \times \frac{1}{\epsilon_b(\mathbf{r})} \boldsymbol{\nabla} \times,$$

$$\boldsymbol{\Theta}_n \equiv \boldsymbol{\nabla} \times d_n(\mathbf{r}) \boldsymbol{\nabla} \times. \tag{2.3}$$

The modal field of the nth microcavity when all other defects are absent, $\mathbf{H}_n(\mathbf{r})$, satisfies

$$(\boldsymbol{\Theta}^b \times \boldsymbol{\Theta}_n)\mathbf{H}_n(\mathbf{r}) = \left(\frac{\omega_n}{c}\right)^2 \mathbf{H}_n(\mathbf{r}). \tag{2.4}$$

The equation for the entire CCW is

$$\boldsymbol{\Theta}\mathbf{H}(\mathbf{r}) = \left(\boldsymbol{\Theta}^b + \sum_n \boldsymbol{\Theta}_n\right)\mathbf{H}(\mathbf{r}) = \left(\frac{\omega}{c}\right)^2 \mathbf{H}(\mathbf{r}). \tag{2.5}$$

Under the weak coupling assumption, we express the total magnetic field $\mathbf{H}(\mathbf{r})$ as a sum of the isolated microcavities magnetic fields:

$$\mathbf{H}(\mathbf{r}) = \sum_n A_n \mathbf{H}_n(\mathbf{r}), \tag{2.6}$$

where $\{A_n\}$ is a set of unknown coefficients, and $\mathbf{H}_n$ satisfies Eq. (2.4). Following the variational procedure used in previous work,[4] we obtain the difference equation for A_n,

$$\sum_n \left\{ \left[\left(\frac{\omega_k}{c} \right)^2 - \left(\frac{\omega}{c} \right)^2 \right] I_{nk} + T'_{n,k} \right\} A_n = 0 \quad \forall\, k, \quad (2.7)$$

where [from Eqs. (2.4) and (2.5)]

$$I_{nm} \equiv \langle \mathbf{H}_n, \mathbf{H}_m \rangle, \quad T'_{n,m} \equiv \left\langle \mathbf{H}_n, \sum_{j \neq m} \mathbf{\Theta}_j \mathbf{H}_m \right\rangle. \quad (2.8)$$

Note that the operator $\mathbf{\Theta}_j$ in Eqs. (2.3) vanishes identically $\forall \mathbf{r}$, except for the spatial location of the jth local defect. Thus, as shown before,[3,4] the dominant T'_{nk} terms in Eq. (2.8) are $T'_{k+1,k}$, $T'_{k-1,k}$, $T'_{k,k}$, and $T'_{k,k\pm2}$, with $|T'_{k,k}|$, $|T'_{k,k\pm2}| \ll |T'_{k\pm1,k}|$. Also, $I_{nm} \equiv \langle \mathbf{H}_n, \mathbf{H}_m \rangle \approx \delta_{nm}$ (I_{nn} is highly dominant). Furthermore, $\omega_k = \omega_0 + \delta\omega_k$ and $\omega_k^2 \approx \omega_0^2 + 2\omega_0 \delta\omega_k$. With these approximations, and keeping only the dominant terms in $I_{mn}, T'_{n,k}$, Eq. (2.7) gets the form

$$\Omega^2 A_k + 2c^{-2}\omega_0 \delta\omega_k A_k + T'_{k-1,k} A_{k-1} + T'_{k+1,k} A_{k+1} = 0 \quad \forall\, k, \quad (2.9a)$$

where

$$\Omega^2 \equiv (\omega_0^2 - \omega^2)/c^2. \quad (2.9b)$$

We shall use Eq. (2.9a) as the basic formulation that governs the propagation of optical signals in nonuniform CCWs. It is important to note that this formulation, based on a tight-binding approximation, holds for CCWs's in which long-range interaction effects can be neglected. This is precisely the meaning of the inequality $|T'_{k,k\pm2}| \ll |T'_{k\pm1,k}|$ used to obtain the formulation in Eq. (2.9a). More $T'_{k,j}$ terms should be kept in the case when long-range interactions are considered,[17] which is not in the scope of the present work.

A. Symmetry Property of $T'_{n,m}$

Note that for a lossless medium, the $\mathbf{\Theta}_j$ operators are real and self-adjoint, and the $\mathbf{H}_n$ fields are real. Thus, $T'_{n,m}$ in Eqs. (2.8) can be rewritten as

$$\begin{aligned} T'_{n,m} &= \sum_{j \neq m} \langle \mathbf{\Theta}_j \mathbf{H}_n, \mathbf{H}_m \rangle = \sum_{j \neq m,n} \langle \mathbf{\Theta}_j \mathbf{H}_n, \mathbf{H}_m \rangle + \langle \mathbf{\Theta}_n \mathbf{H}_n, \mathbf{H}_m \rangle \\ &= \sum_{j \neq n} \langle \mathbf{\Theta}_j \mathbf{H}_n, \mathbf{H}_m \rangle + \langle \mathbf{\Theta}_n \mathbf{H}_n, \mathbf{H}_m \rangle - \langle \mathbf{\Theta}_m \mathbf{H}_n, \mathbf{H}_m \rangle \\ &= T'_{m,n} + \langle \mathbf{\Theta}_n \mathbf{H}_n, \mathbf{H}_m \rangle - \langle \mathbf{\Theta}_m \mathbf{H}_m, \mathbf{H}_n \rangle \\ &\qquad (\mathbf{H}_n, \mathbf{\Theta}_j \text{ real and self-adjoint}). \quad (2.10) \end{aligned}$$

Therefore

$$T'_{n,m} + \langle \mathbf{\Theta}_m \mathbf{H}_m, \mathbf{H}_n \rangle = T'_{m,n} + \langle \mathbf{\Theta}_n \mathbf{H}_n, \mathbf{H}_m \rangle. \quad (2.11)$$

Thus, as long as the mth and nth cavities belong to the same uniform waveguide, we have

$$T'_{n,m} = T'_{m,n}. \quad (2.12)$$

This property is used in the subsequent derivations.

B. Special Case: the Limit of the Uniform Coupled-Cavity Waveguide

For all k we have $\delta\omega_k = 0$ and $T'_{k-1,k} = T'_{k+1,k} = \tau$, so Eq. (2.9a) reduces to

$$\Omega^2 A_k + \tau(A_{k-1} + A_{k+1}) = 0 \quad \forall\, k. \quad (2.13)$$

Substituting a solution of the form

$$A_k = e^{i\beta k}, \quad (2.14)$$

Eq. (2.13) produces the known dispersion relation

$$\Omega^2 = -2\tau \cos\beta. \quad (2.15)$$

Approximating

$$\Omega^2 = \frac{1}{c^2}(\omega_0 - \omega)(\omega_0 + \omega) \approx \frac{2\omega_0}{c^2}(\omega_0 - \omega), \quad (2.16)$$

we obtain from Eq. (2.15)

$$\omega - \omega_0 = (\Delta\omega/2)\cos\beta, \quad (2.17)$$

where the CCW transmission bandwidth $\Delta\omega$ and τ are related via

$$\tau = \frac{\omega_0 \Delta\omega}{2c^2}. \quad (2.18)$$

3. PROPAGATION IN NONUNIFORM COUPLED-CAVITY WAVEGUIDES

Here we study the case of a nonuniform CCW consisting of two uniform CCWs connected in series, as shown schematically in Fig. 1. For convenience, we start in Subsection 3.A with the simplest case where both have the same central frequency and they differ in their bandwidth. After establishing this case in Subsection 3.B we generalize it to the case of CCWs having a different central frequency and different bandwidth.

A. Two Coupled-Cavity Waveguides with the Same Central Frequency

Here we study the case of a nonuniform CCW that consists of two uniform CCWs, both having identical microcavities. Thus they possess the same central frequency, but differ in their frequency bandwidths due to different intercavity spacings. We have $\Delta\omega_1$ obtained with intercavity spacing b_1 for the left waveguide ($k \leqslant 0$) and $\Delta\omega_2$ obtained with intercavity spacing b_2 for the right waveguide ($k > 0$). Referring to the configuration in Fig. 1, this case is characterized by solid circles [Fig. 1(a)] or rings [Fig. 1(b)] with k-independent radii.

From the problem geometry, and from the fact that Eq. (2.12) holds separately within each waveguide, it follows that

$$\delta\omega_k = 0 \quad \forall\, k, \quad (3.1a)$$

$$T'_{k-1,k} = \begin{cases} \tau_1 & \forall k \leqslant 0 \\ \tau_2 & \forall k \geqslant 1 \end{cases}. \quad (3.1b)$$

Furthermore, because of the results in Subsection 2.A, we have

$$T'_{m,n} = T'_{n,m} \quad \forall\, m,n \leqslant 0 \quad \text{or } m,n \geqslant 0, \quad (3.1c)$$

$$T'_{k-1,k} = T'_{k+1,k} = \begin{cases} \tau_1 & \forall k \leqslant -1 \\ \tau_2 & \forall k \geqslant 2 \end{cases}. \quad (3.1d)$$

Equation (2.9a) still governs the modal propagation along the combined CCW. Because of the property jump between $k=0$ and $k=1$, we write a solution of the form:

$$A_k = \begin{cases} e^{i\beta_1 k} + \Gamma e^{-i\beta_1 k}, & \forall k \leqslant 0 \\ T e^{i\beta_2 k}, & \forall k \geqslant 1 \end{cases}. \tag{3.2}$$

Substituting this into Eq. (2.9a), and using Eqs. (3.1a), (3.1b), and (3.1c), we obtain, respectively, for $k \leqslant -1$ and for $k \geqslant 2$

$$\Omega^2(e^{i\beta_1 k} + \Gamma e^{-i\beta_1 k}) + 2\tau_1 \cos\beta_1 (e^{i\beta_1 k} + \Gamma e^{-i\beta_1 k}) = 0, \quad \forall k \leqslant -1, \tag{3.3a}$$

$$\Omega^2 T e^{i\beta_2 k} + 2\tau_2 T \cos\beta_2 e^{i\beta_2 k} = 0, \quad \forall k \geqslant 2, \tag{3.3b}$$

from which we obtain the two perfect CCW conventional dispersion relations, similar in form to Eq. (2.15):

$$\Omega^2 = -2\tau_1 \cos\beta_1, \quad \Omega^2 = -2\tau_2 \cos\beta_2. \tag{3.4}$$

Note that τ_1, τ_2 are related to the respective bandwidths $\Delta\omega_1, \Delta\omega_2$ of the two uniform sections, in a manner similar to Eq. (2.18). Therefore, for the waves in the two sections, we have

$$\omega - \omega_0 = (\Delta\omega_1/2)\cos\beta_1, \tag{3.5a}$$

$$\omega - \omega_0 = (\Delta\omega_2/2)\cos\beta_2, \tag{3.5b}$$

where

$$\Delta\omega_{1,2} = 2c^2\tau_{1,2}/\omega_0. \tag{3.6}$$

The interesting physics takes place at $k=0$ and $k=1$:

$$\Omega^2 A_0 + T'_{-1,0}A_{-1} + T'_{1,0}A_1 = 0 \quad (k=0), \tag{3.7a}$$

$$\Omega^2 A_1 + T'_{0,1}A_0 + T'_{2,1}A_2 = 0 \quad (k=1). \tag{3.7b}$$

Substituting Eq. (3.2) for A_1 and A_2 and solving for Γ and T using Eqs. (3.1a), (3.1b), (3.1c), and (3.1d) [note that with Eqs. (3.4) we have $\Omega^2 + \tau_n e^{i\beta_n} = -\tau_n e^{-i\beta_n}$, $n=1,2$], we obtain

$$T = 1 + \Gamma, \quad \Gamma(\omega) = -\frac{\tau_1 e^{-\beta_1} - \tau_2 e^{-i\beta_2}}{\tau_1 e^{i\beta_1} - \tau_2 e^{-i\beta_2}} = -\frac{\tau_1 e^{i\beta_1} - \tau_2 e^{i\beta_2}}{\tau_1 e^{-i\beta_1} - \tau_2 e^{i\beta_2}}. \tag{3.8}$$

The expression for Γ can be further simplified by using the exact dispersion relations in Eqs. (3.4) and the bandwidths' expression in Eq. (3.6). The result is

$$\Gamma(\omega) = -\frac{\Delta\omega_2\sqrt{1-\left(\frac{\omega-\omega_0}{\Delta\omega_2/2}\right)^2} - \Delta\omega_1\sqrt{1-\left(\frac{\omega-\omega_0}{\Delta\omega_1/2}\right)^2}}{\Delta\omega_2\sqrt{1-\left(\frac{\omega-\omega_0}{\Delta\omega_2/2}\right)^2} + \Delta\omega_1\sqrt{1-\left(\frac{\omega-\omega_0}{\Delta\omega_1/2}\right)^2}}. \tag{3.9}$$

Equation (3.9) gives the transmission and reflection coefficients as functions of frequency, within the entire frequency bands of both CCWs. Its structure has the same form as that of the well-known Fresnel reflection coefficient. At the central frequency ($\omega=\omega_0$), we have

$$\Gamma(\omega_0) = \frac{\Delta\omega_2 - \Delta\omega_1}{\Delta\omega_2 + \Delta\omega_1}. \tag{3.10}$$

This last result is identical with the Fresnel reflection coefficient, with $\Delta\omega$ replacing the traditional wave impedance. Furthermore, it is seen from Eq. (3.9) that if the frequency ω exits the transmission band of one of the CCWs, the reflection coefficient becomes a complex number with unity magnitude ($\Delta\omega_i$ is the total bandwidth of the ith CCW), similar to the total internal reflections phenomenon.

B. Two Uniform Cavity-Coupled Waveguides with Different Central Frequencies and Different Bandwidths

This case is identical to the previous one, except that the first CCW (occupying indices $k \leqslant 0$) central frequency is $\omega_{01}=\omega_0$, whereas the second CCW (occupying indices $k \geqslant 1$) central frequency is $\omega_{02}=\omega_0+\delta\omega_0$, for all $k \geqslant 1$. The system is described in Fig. 1. Thus Eq. (3.1a) is replaced by

$$\delta\omega_k = \begin{cases} 0, & \forall k \leqslant 0 \\ \delta\omega_0 = \Delta_0 c^2/2\omega_0, & \forall k \geqslant 1 \end{cases}, \tag{3.11}$$

where the parameter Δ_0 here represents the central frequency difference between the left and right CCWs, defined for convenience in the subsequent derivations. Also, the second equality in Eq. (3.1b) holds now for $k \geqslant 2$, and Eq. (3.1c) still holds with the domains of m,n changed to $\forall m,n \leqslant 0$, or $m,n \geqslant 1$. Thus, in this more general configuration,

$$T'_{0,1} \neq T'_{1,0} \neq \tau_2. \tag{3.12}$$

This inequality is important in subsequent derivations. Finally, Eq. (3.1d) is unchanged.

We can now follow exactly the same procedure of the previous case in Subsection 3.A. The modal amplitudes form in Eq. (3.2) still holds, and Eqs. (3.3a) and (3.3b) now read as

$$\Omega^2(e^{i\beta_1 k} + \Gamma e^{-i\beta_1 k}) + 2\tau_1 \cos\beta_1 (e^{i\beta_1 k} + \Gamma e^{-i\beta_1 k}) = 0, \quad \forall k \leqslant -1, \tag{3.13a}$$

$$(\Omega^2 + \Delta_0) T e^{i\beta_2 k} + 2\tau_2 T \cos\beta_2 e^{i\beta_2 k} = 0, \quad \forall k \geqslant 2, \tag{3.13b}$$

from which we obtain the two perfect CCW conventional dispersion relations:

$$\Omega^2 = -2\tau_1 \cos\beta_1, \quad \Omega^2 + \Delta_0 = -2\tau_2 \cos\beta_2. \tag{3.14}$$

The parameters τ_1, τ_2 are related to the respective CCWs bandwidths via the same expressions as before, Eq. (3.6). Using the same procedure that we used in Eqs. (3.4)–(3.6), we obtain

$$\omega - \omega_{01} = (\Delta\omega_1/2)\cos\beta_1, \tag{3.15a}$$

$$\omega - \omega_{02} = (\Delta\omega_2/2)\cos\beta_2, \quad (\omega_{02} = \omega_{01} + \delta\omega_0), \tag{3.15b}$$

where Eq. (3.6) connecting bandwidths to $\tau_{1,2}$ holds. Likewise, Eq. (3.7a) still holds, and a corresponding slight modification applies to Eq. (3.7b): The Ω^2 term is replaced by $\Omega^2+\Delta_0$. Continuing along the same lines, we obtain for

the transmission and reflection coefficients [Eq. (3.12) should be considered]

$$T = \frac{T'_{0,1}}{\tau_2}(1+\Gamma), \quad \Gamma(\omega) = -\frac{\tau_1 e^{i\beta_1} - \alpha\tau_2 e^{i\beta_2}}{\tau_1 e^{-i\beta_1} - \alpha\tau_2 e^{i\beta_2}}, \tag{3.16a}$$

where α is a factor indicating the degree to which the $T'_{1,0}, T'_{0,1}$ mismatch τ_2:

$$\alpha = \frac{T'_{1,0}T'_{0,1}}{\tau_2^2}. \tag{3.16b}$$

This last result can be rewritten in terms of the frequency ω:

$$\Gamma(\omega) = -\frac{2\alpha(\omega_{02}-\omega) - 2(\omega_{01}-\omega) + i\left[\Delta\omega_1 s_1 - \Delta\omega_2\alpha\dfrac{\omega_{02}}{\omega_{01}}s_2\right]}{2\alpha(\omega_{02}-\omega) - 2(\omega_{01}-\omega) - i\left[\Delta\omega_1 s_1 + \Delta\omega_2\alpha\dfrac{\omega_{02}}{\omega_{01}}s_2\right]}, \tag{3.17a}$$

where $\Delta\omega_1, \Delta\omega_2$ are the bandwidths of the first and second CCWs, ω_{01}, ω_{02} are their respective central frequencies [see Eqs. (3.15a) and (3.15b) and discussion before Eq. (3.11)], and s_1, s_2 are given by

$$s_{1,2} = \sqrt{1 - \left(\frac{\omega - \omega_{01,2}}{\Delta\omega_{12}/2}\right)^2}. \tag{3.17b}$$

Note that if the central frequencies of the first and second CCWs are identical, then $\alpha = 1$, $\omega_{01} = \omega_{02}$, so the expression for Γ and T reduce to the simpler ones developed in Subsection 3.A.

C. Comment on the Symmetry Properties of Γ and T and an Analogy

Let $\vec{\Gamma}$ ($\overleftarrow{\Gamma}$) be the reflection coefficient that applies for a wave propagating rightward (leftward) and hitting the discontinuity from the left (right). Likewise, let $\mathbf{T}$ ($\overleftarrow{\mathbf{T}}$) be the corresponding transmission coefficients. From the results of Subsection 3.A it follows that for the case of two CCWs with identical central frequencies, one obtains $\mathbf{\Gamma} = -\mathbf{\Gamma}$ and $\mathbf{T} + \mathbf{T} = 2$. However, if the central frequencies are different (see Subsection 3.B), this symmetry is lost. Therefore, the configuration of two CCWs with identical central frequencies is analogous to the interface between two conventional waveguides that possess the same cross-section geometries (and free space can be seen as a special case). This analogy is further motivated by noting the identity $T = 1 + \Gamma$ [see Eqs. (3.8)] that holds in general for uniform geometry connections. The configuration of two CCWs with different central frequencies can be seen as an analog of waveguides with different cross-section geometries.

D. Effect of Loss

Since the basic building block of the CCWs is a high-Q resonator, loss can be an important factor affecting the CCW performance. There are two main types of losses: material (dielectric) losses resulting either from ohmic dissipation (conduction) or from dissipative polarization processes of the dielectric material, and scattering losses that are caused mainly by unavoidable geometric imperfections. The former can be rigorously represented by adding an imaginary component to the dielectric property $\epsilon_r(\mathbf{r}) = \epsilon'_r(\mathbf{r}) + i\epsilon''_r(\mathbf{r})$.[18] The latter are more difficult to model, but they can heuristically be represented by a modification of ϵ''. The complex ϵ can now be inserted into the wave operator $\mathbf{\Theta}$, and the analysis in this paper can in principle be repeated. Note, however, that there are several subtle issues in this approach. With complex ϵ the wave operator $\mathbf{\Theta}$ is no longer self-adjoint, so the variational procedure leading from the wave Eq. (2.5) to the difference Eq. (2.9a) does not hold. Nevertheless, it has been shown[11] that by applying a Galerkin projection procedure, one can obtain a difference equation for a CCW in non-self-adjoint conditions. Furthermore, performing such an analysis one can see that the difference equation has exactly the same form as Eq. (2.9a) with dominant terms as before, except for the addition of complex components to the coefficients $T'_{k\pm1,k}$ [as evidenced from Eqs. (2.8)], and at the expense of losing some of their symmetry properties (see Subsection 2.A). It is anticipated, therefore, that the case of lossy CCW is analytically identical to the lossless one, with the replacement of $\tau_{1,2}$ in Eqs. (3.8) or Eqs. (3.16) by their complex counterparts (note that $\tau_1 = T'_{k\pm1,k}$ for $k < 0$ and $\tau_2 = T'_{k\pm1,k}$ for $k > 1$). Thus, for example, the equality $T = 1 + \Gamma$ discussed above still holds, but it should be emphasized that it does not necessarily mean an energy conservation; rather, in light of the analogies discussed above, it conveys continuity conditions for the fields. A detailed investigation of the ramifications of such results is beyond the scope of the present paper.

4. MATCHING TWO COUPLED-CAVITY WAVEGUIDES BY AN INTERMEDIATE SECTION

A. General Expressions

We wish to connect two different CCWs and reduce the discontinuity backreflections to a minimum for a prescribed frequency. One possible way to achieve this goal is to insert in series a finite-length intermediate section between the two CCWs, as shown schematically in Fig. 2.

The leftmost and rightmost CCWs have infinite length and they occupy microcavity indices $k \leqslant 0$ and $k \geqslant M+1$, respectively, while the intermediate section consists of M

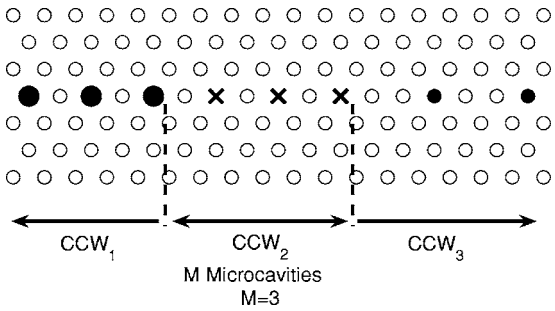

Fig. 2. Two different CCWs connected in series, matched by an intermediate section with M microcavities.

microcavities. Counting from left to right, the ith CCW is termed here by CCW_i ($i=1,2,3$), and it possesses a central frequency, bandwidth, and propagation constant ω_{0i}, $\Delta\omega_i$, and $\beta_i(\omega)$, respectively. Assume now that the system is excited by an optical signal that propagates in CCW_1 from left to right. The incident and reflected modal amplitudes are given, respectively, by

$$A_k^i = e^{i\beta_1 k}, \quad A_k^r = R\, e^{-i\beta_1 k}, \quad k \leqslant 0, \tag{4.1}$$

where R represents the reflection from the combined CCWs' system, as seen from within CCW_1, and as measured with respect to the reference microcavity $k=0$. Summing up all contributions for the field at $k=0$, due to the multiple reflections that take place within CCW_2, we get for R

$$R = \Gamma_{12} + T_{12}T_{21}\Gamma_{23}\, e^{2i\beta_2 M}\sum_{n=0}^{\infty}[e^{2i\beta_2 M}\Gamma_{23}\Gamma_{21}]^n. \tag{4.2}$$

Here Γ_{ij} is the local Fresnel-like reflection coefficient for the modal amplitudes of a wave propagating in CCW_i and hitting the interface with CCW_j. Likewise, T_{ij} is the local transmission coefficient for a wave passing from CCW_i to CCW_j. Both Γ_{ij} and T_{ij} were developed in Section 3.

Summing the geometric series in Eq. (4.2), we obtain the CCW analog of a classical result:

$$R = \frac{\Gamma_{12} - \Gamma_{23}[\Gamma_{12}\Gamma_{21} - T_{12}T_{21}]e^{2i\beta_2 M}}{1 - \Gamma_{23}\Gamma_{21}\, e^{2i\beta_2 M}}. \tag{4.3}$$

From this last result it is seen that perfect matching between CCW_1 and CCW_3, corresponding to $R=0$, is obtained when the CCWs' parameters satisfy

$$\Gamma_{12} = \Gamma_{23}[\Gamma_{12}\Gamma_{21} - T_{21}T_{21}]e^{2i\beta_2 M}. \tag{4.4}$$

We now demonstrate a simple and illuminating case for which the above condition can be satisfied.

B. λ/4 Plate Analog

Consider the simplified configuration of two CCWs (namely, CCW_1 and CCW_3) with the same central frequency and different bandwidths. Thus $\omega_{01}=\omega_{03}$ and $\Delta\omega_1 \neq \Delta\omega_3$. We would like to match these CCWs at their central frequency. Referring back to the discussion in Subsection 3.C, an analogy with the problem of matching two waveguides with an identical cross-section geometry is suggested. Thus, we anticipate that an intermediate matching section CCW_2 with the same central frequency $\omega_{01}=\omega_{01}=\omega_{03}$ can be used to satisfy the condition set by Eq. (4.4), provided that the appropriate section length (M) and bandwidth ($\Delta\omega_2$) are chosen. Using the ensuing symmetry properties $\Gamma_{ij}=-\Gamma_{ji}$ and $T_{ij}=2-T_{ji}$ (see Subsection 3.C), Eq. (4.4) reduces to

$$\Gamma_{12} = -\Gamma_{23}\, e^{2i\beta_2 M}. \tag{4.5}$$

However, at the central frequency we have $\beta_i=\pi/2$, and by using Eq. (3.10) it is easily seen that matching at the central frequency is obtained for

$$M = 2n+1 \text{ with } n = 0,1,2,\ldots, \quad \Delta\omega_2 = \sqrt{\Delta\omega_1\Delta\omega_3}. \tag{4.6}$$

Thus, perfect matching can be obtained by inserting an intermediate section with an equivalent optical length of $\lambda/4$ (as implied by the fact that $\beta=\pi/2$) and with a bandwidth given by the geometric mean. The perfect analogy with the well-known quarter-wavelength plate matching, obtained by replacing the wave impedance with the CCWs bandwidths, is apparent (see also discussion at the end of Subsections 3.A and 3.C). Note that the case of $M=1$, corresponding to a single microcavity matching section, is a legitimate solution. Here the corresponding bandwidth is achieved by choosing the correct intercavity distances. The efficacy of this result will be demonstrated in Section 5.

5. NUMERICAL EXAMPLES

Here we shall solve numerically several configurations consisting of uniform CCWs connected in series as schematized in Figs. 1 and 2, calculate the respective reflection and transmission coefficients, and check the results against the analytic predictions of the previous sections. The theory developed in previous sections holds for CCWs in 2D and 3D crystals as well. However, since each CCW should consist of several microcavities (say, four or five), and the intercavity distance must be two PhC unit cells or more, the numerical size of the problem becomes excessively large for full 3D simulations. Thus, we shall limit this section to examples of 2D geometries only. Specifically, we shall use the hexagonal PhC lattice that is used, for example, in Refs. 3 and 4. The PhC is made of dielectric cylinders with $\epsilon_r=8.41$, radii of 0.6, and cylinder spacing of 4 (all in arbitrary length units). The resulting PhC possesses a bandgap in the range of $7.5 \leqslant \lambda \leqslant 10.5$ in arbitrary length units. A microcavity created by removing a single post resonates at $\lambda_0=9.058$. By slightly changing the radii of the microcavity's six closest neighboring cylinders, the resonant wavelength can be tuned to any desired value between 8.4 and 9.8 in arbitrary length units (see examples in Ref. 4).

We start by comparing the results of Subsection 3.A with numerical simulations. The combined CCWs consisting of uniform sections built of microcavities with identical resonant wavelengths are shown in Fig. 3. The intercavity spacing in the left and right CCWs is three and two unit cells, respectively, yielding transmission bandwidths of $\Delta\lambda=0.118$ and 0.5, both centered around $\lambda_0=9.058$.[3] The system is excited by an incident TM plane wave, propagating from left to right. The rightmost section of the combined CCW (the uniform CCW that occupies indices $k \geqslant 1$) is matched to the free space at the right end of the crystal by using a matching dielectric post as described in previous works concerning matching to free space.[19,20] This matching reduces the backreflections in the rightmost output terminal of the CCW to a few percent, so one can assume that the modal propagation in this section ($k \geqslant 1$) consists of essentially a right-propagating wave. Thus the left-propagating mode in the left section ($k \leqslant 0$) results only from the reflections that take place across the CCW discontinuity at $k=0$. We have

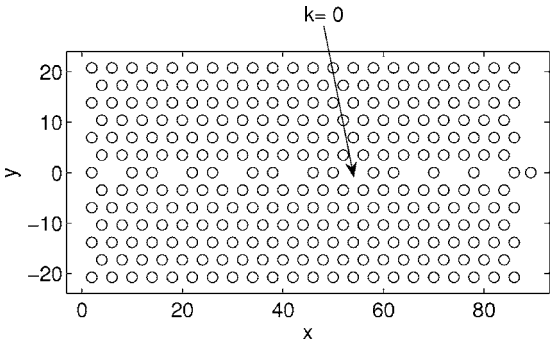

Fig. 3. Two sections with identical central frequencies and different bandwidths. All the dielectric cylinders in the crystal are of radius 0.6 and $\epsilon_r=8.41$. The crystal spacing is $a=4$. The dielectric cylinder used to match the system output to free space is seen on the right, external to the structure. Its material is identical to that of the PhC. Its radius is 0.4 and its x coordinate is 3.3 to the right of the rightmost cylinder in the crystal.[19]

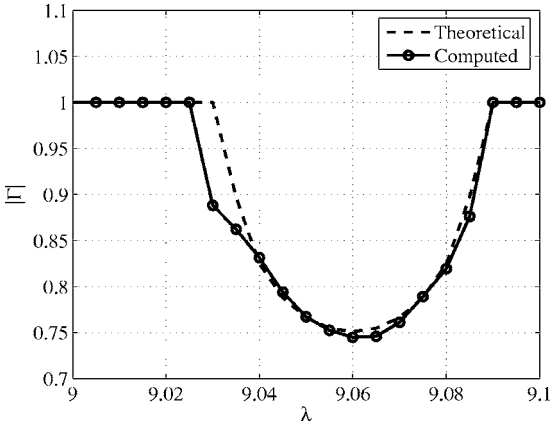

Fig. 4. Reflection coefficient obtained for the configuration described in Fig. 3.

used the method described in Appendix A to compute the amplitudes of the left- and right-propagating waves in this section. Their ratio is the reflection coefficient Γ. Figure 4 compares this numerically computed Γ with the one predicted by Eq. (3.9). Quite a good agreement is seen (note the vertical scale). The deviations between the two lines at the left side of the graph are attributed to numerical inaccuracy due to the relatively small number of microcavities used.

Figure 5 shows a combined system of two CCWs differing in both the central frequency and the bandwidth. It is essentially the same configuration as that of the previous example, except that the resonant wavelength of the left CCWs is increased to $\lambda_1=9.15$. This is obtained by slightly increasing the radius of the six closest neighbors of the corresponding cavities from $r=0.6$ to $r=0.64$.[4] The resulting reflection coefficient has been computed numerically and in Fig. 6 it is compared with the analytic prediction of Eqs. (3.17). Again, quite a good agreement is seen (note the vertical scale).

The quarter-wavelength analog prediction of Subsection 4.B is now examined. The combined system is shown in Fig. 7. We use the same PhC background structure as in the previous examples. Also, for CCW_2 and CCW_3 we use the same cavity structure and intercavity spacing as used in the example of Fig. 3, namely, bandwidths $\Delta\lambda_2=0.118$ and $\Delta\lambda_3=0.5$, respectively, and a resonant wavelength $\lambda_0=9.058$ for both. We use CCW_2 as an intermediate matching section, with $M=1$. CCW_1 consists of microcavities created again by a removal of a dielectric cylinder, with an intercavity spacing of four unit cells. This yields an extremely narrow bandwidth. By increasing the radius of the cylinders in the second ring around each microcavity to $r=0.66$, we have increased the cavities' mutual coupling, thus achieving a larger bandwidth of $\Delta\lambda_1=0.025$. This addition of dielectric material, however, caused an upward shift of the resonant wavelength to beyond 9.07. Thus, we have slightly decreased the ra-

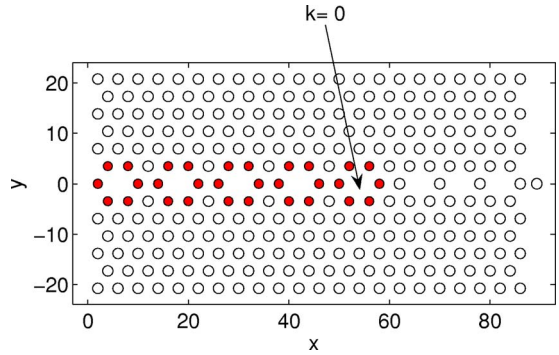

Fig. 5. (Color online) Two sections with different central frequencies and bandwidths. The parameters are the same as in the previous example, except for the shaded circles representing dielectric cylinders of the same material but of radius 0.64. The dielectric cylinder used to match the system output to free space is seen on the right. It has the same parameters as in the previous example.

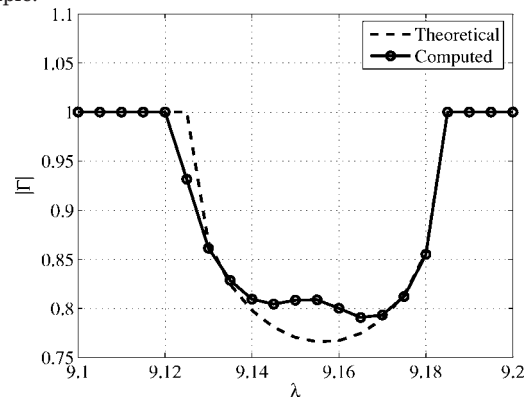

Fig. 6. Reflection coefficient obtained for the configuration described in Fig. 5.

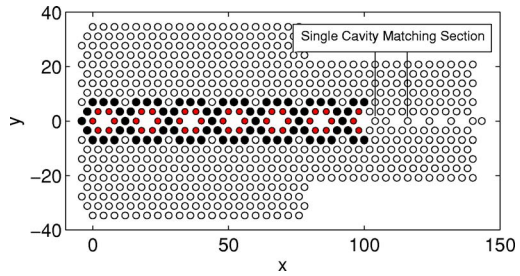

Fig. 7. (Color online) Quarter-wavelength plate analog of two different CCWs connected in series, matched by an intermediate section of a single microcavity. The crystal parameters are the same as in the previous examples, except for the solid large circle and shaded small circles, representing dielectric cylinders of the same material but of radius 0.66 and 0.587, respectively.

dius of each cavity's six closest cylinders from $r=0.6$ to $r=0.587$.[4] The final result is that CCW_1's central wavelength λ_1 is returned to 9.058, and its bandwidth $\Delta\lambda_1$ is tuned to 0.025. The three bandwidths and the intermediate section length now approximately satisfy the conditions set by the geometric mean in Eqs. (4.6), with $n=0$. Note that since the rightmost cavity of CCW_1 has larger dielectric cylinders of radius 0.66 only on its left side, the corresponding resonant tuning is achieved by a radius decrease of only three neighbors instead of six. The system was excited by an incident plane wave from its left side. The reflection coefficient of the combined system of CCW_2 and CCW_3, as seen from within CCW_1, has been computed using the method outlined in Appendix A. The result is shown in Fig. 8. It is seen that the reflection coefficient is ~0.1 near the resonant wavelength, and thus a good matching is achieved. Figure 9 shows the phase of the transmitted field in CCW_3 right after the matching section (cavity 9 from the left) relative to the phase of the incident field in CCW_1 far from the matching section (cavity 4 from the left). It is seen that the transmission coefficient across the matching section consists essentially of a group delay; the phase is quite linear within the transmission band, with the slope indicating a group delay due to the propagation from cavity 4 to cavity 9.

Finally, a comment about the numerical accuracy is in order. Each example in this section consists of essentially two computational steps. First, we obtain the total fields in the PhC system by a full-wave solution of Maxwell's equations (using the moment-method-based multifilament code[3,21]). Then, the method outlined in Appendix A is used to predict the reflection coefficient. In the former step, a systematic check of the error in satisfying the boundary conditions is invoked. The maximal relative error is a fraction of a percent for **E** and is of the order of 1% for **H**. Thus, we surmise that the field solutions are accurate of the order of a percent. Then the error in predicting Γ is essentially correlated to the residual error obtained in the procedure discussed in Appendix A. This error was a fraction of a percent in the examples shown in Figs. 4 and 6 and of the order of 20% in the example shown in Figs. 8 and 9. A larger number of cavities and a better cavity isolation from the free space (i.e., reduction of the radiation loss from each cavity) can improve this accuracy. The latter requires an increase of the number of the PhC rows above and below the CCWs. Note, however, that the total number of dielectric cylinders in this problem is 631, yielding a moment-method matrix with more then 15,000 unknowns (24 unknown current filaments are needed for each cylinder[21]). Thus, the numerical size of the problem is already excessively large, and increasing it further may cause numerical errors and instabilities to take over.

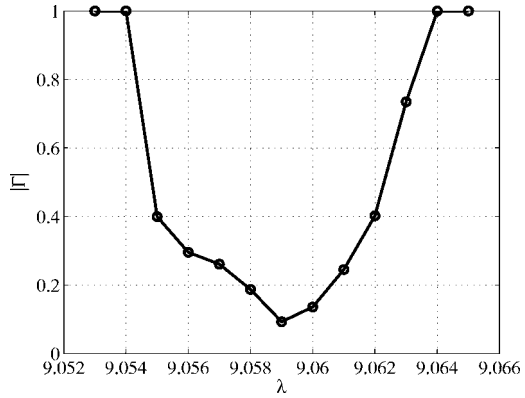

Fig. 8. Reflection coefficient obtained by using a single-cavity intermediate matching section.

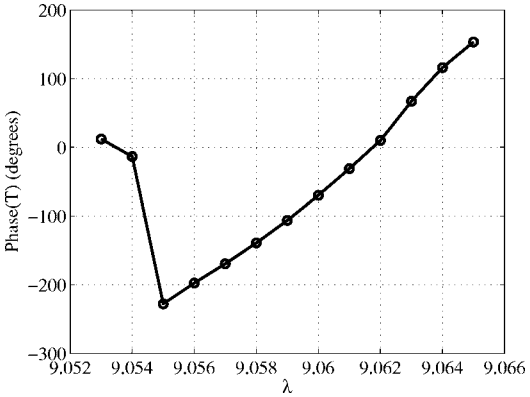

Fig. 9. Phase of the transmitted field in CCW_3 relative to the phase of the incident field in CCW_1.

6. CONCLUSIONS

Using a formulation developed from the tight-binding theory, an equation governing the propagation in nonuniform CCWs has been developed. It is shown that analytic expressions for reflection by and transmission through discontinuity in the properties of a CCW can be derived from the new theory. These expressions resemble in many ways celebrated results that apply to propagation in waveguides and TEM transmission lines, with the replacement of the wave impedances by the corresponding CCWs' bandwidth. These new results can serve as the basis for developing network theory for CCWs' assemblies. A simple example of matching two CCWs with the use of an intermediate CCW section is demonstrated, and an analogy to the well-known quarter-wavelength plate is pointed out. The analytic results are checked against numerical simulations, showing quite a good agreement between them. It is anticipated that the present results can be of help in analyzing systems where multiply connected CCWs are used.

APPENDIX A: COMPUTING THE REFLECTION COEFFICIENT FROM NUMERICAL DATA

Consider a CCW comprising $N+1$ microcavities. Let $\{E_n\}_{n=0,\ldots N}$ be a given set of numerical measurements of the electric field data in the microcavities. These are given generally by $E_n=E(\mathbf{r}_c+n\mathbf{b})$ where $\mathbf{r}_c$ is a reference point chosen within the first cavity, at a location where the amplitude of the cavity excitation can be conveniently measured (for symmetric cavity modes it is the cavity center), and $\mathbf{b}$ is the intercavity spacing vector. We assume that the field in the nth cavity is given by $a^+e^{i\beta n}+a^-e^{-i\beta n}$, where β is the propagation constant and a^+ and a^- denote the amplitudes of the propagating and reflected waves,

respectively. Generally, these amplitudes depend on β. The relation among the electric field, the amplitudes, and β can be expressed via

$$\begin{bmatrix} 1 & 1 \\ e^{i\beta} & e^{-i\beta} \\ e^{i2\beta} & e^{-i2\beta} \\ \vdots & \vdots \\ e^{iN\beta} & e^{-iN\beta} \end{bmatrix} \begin{bmatrix} a^{+}(\beta) \\ a^{-}(\beta) \end{bmatrix} = \begin{bmatrix} E_0 \\ E_1 \\ \vdots \\ E_N \end{bmatrix}. \tag{A1}$$

The procedure for computing β and the amplitudes $a^{\pm}(\beta)$ is the following one-dimensional minimization procedure. Numerically search for β, for which the solution of Eq. (A1) in the least-squares sense, possesses the minimal residual error. The corresponding $a^{\pm}(\beta)$ are the ones we look for. Naturally, the reflection coefficient is determined as $\Gamma = a^{-}/a^{+}$.

B. Z. Steinberg, steinber@eng.tau.ac.il; A. Boag, boag@eng.tau.ac.il.

REFERENCES

1. A. Yariv, Y. Xu, R. K. Lee, and A. Scherer, "Coupled-resonator optical waveguide: a proposal and analysis," Opt. Lett. **24**, 711–713 (1999).
2. M. Bayindir, B. Temelkuran, and E. Ozbay, "Tight-binding description of the coupled defect modes in three-dimensional photonic crystals," Phys. Rev. Lett. **84**, 2140–2143 (2000).
3. A. Boag and B. Z. Steinberg, "Narrow-band microcavity waveguides in photonic crystals," J. Opt. Soc. Am. A **18**, 2799–2805 (2001).
4. B. Z. Steinberg, A. Boag, and R. Lisitsin, "Sensitivity analysis of narrow-band photonic crystal filters and waveguides to structure variations and inaccuracy," J. Opt. Soc. Am. A **20**, 138–146 (2003).
5. J. K. S. Poon, J. Scheuer, S. Mookherjea, G. T. Paloczi, Y. Huang, and A. Yariv, "Matrix analysis of microring coupled-resonator optical waveguides," Opt. Express **12**, 90–103 (2004).
6. D. N. Christodoulides and N. K. Efremidis, "Discrete temporal solitons along a chain of nonlinear coupled microcavities embedded in photonic crystals," Opt. Lett. **27**, 568–570 (2002).
7. S. Mookherjea and A. Yariv, "Second-harmonic generation with pulses in a coupled-resonator optical waveguide," Phys. Rev. E **65**, 026607 (2002).
8. S. Mookherjea and A. Yariv, "Optical pulse propagation and holographic storage in a coupled-resonator optical waveguide," Phys. Rev. E **64**, 066602 (2001).
9. S. Mookherjea and A. Yariv, "Pulse propagation in a coupled-resonator optical waveguide to all orders of dispersion," Phys. Rev. E **65**, 056601 (2002).
10. J. K. S. Poon, J. Scheuer, Y. Xu, and A. Yariv, "Designing coupled-resonator optical waveguide delay lines," J. Opt. Soc. Am. B **21**, 1665–1673 (2004).
11. B. Z. Steinberg, "Rotating photonic crystals: a medium for compact optical gyroscopes," Phys. Rev. E **71**, 056621–7 (2005).
12. O. Painter, J. Vuckovic, and A. Scherer, "Defect modes of a two-dimensional photonic crystal in an optically thin dielectric slab," J. Opt. Soc. Am. B **16**, 275–285 (1999).
13. T. Yoshie, J. Vuckovic, A. Scherer, H. Chen, and D. Deppe, "High quality two-dimensional photonic crystal slab cavities," Appl. Phys. Lett. **79**, 4289–4291 (2001).
14. B. S. Song, S. Noda, and T. Asano, "Photonic devices based on in-plane hetero photonic crystals," Science **300**, 1537 (2003).
15. B. S. Song, S. Noda, T. Asano, and Y. Akahane, "Ultra-high-Q photonic double heterostructure nanocavity," Nat. Mater. **4**, 207–210 (2005).
16. J. D. Joannopoulos, R. D. Meade, and J. N. Winn, *Photonic Crystals: Molding the Flow of Light* (Princeton U. Press, 1995).
17. S. F. Mingaleev and Y. S. Kivshar, "Effective equations for photonic-crystal waveguides and circuits," Opt. Lett. **27**, 231–233 (2002).
18. J. D. Jackson, *Classical Electrodynamics*, 2nd ed. (Wiley 1975).
19. B. Z. Steinberg, A. Boag, and O. Hershkoviz, "Substructuring approach to optimization of matching for photonic crystal waveguides," Microwave Opt. Technol. Lett. (to be published).
20. A. Boag, B. Z. Steinberg, and O. Bushmakin, "Matching of narrow band photonic crystal filters and waveguides to free space and dielectric waveguides," Presented at 2003 IEEE AP-S International Symposium and USNC/CNC/URSI National Radio Science Meeting, Columbus, Ohio, 22–27 June 2003.
21. A. Boag, Y. Leviatan, and A. Boag, "Analysis of two dimensional electromagnetic scattering from a periodic grating of cylinders using a hybrid current model," Radio Sci. **23**, 612–624 (1988).